doi:10.1093/brain/awab058 BRAIN 2021: Page 1 of 15 | 1

BRAIN
A JOURNAL OF NEUROLOGY

Photo-oxygenation by a biocompatible catalyst reduces amyloid-β levels in Alzheimer's disease mice

Shuta Ozawa,[1,†] Yukiko Hori,[1,†] Yusuke Shimizu,[2,†] Atsuhiko Taniguchi,[2,‡] Takanobu Suzuki,[1] Wenbo Wang,[1] Yung Wen Chiu,[1] Reiko Koike,[3] Satoshi Yokoshima,[3] Tohru Fukuyama,[3] Sho Takatori,[1] Youhei Sohma,[2] Motomu Kanai[2] and Taisuke Tomita[1]

[†]These authors contributed equally to this work.

Amyloid formation and the deposition of the amyloid-β peptide are hallmarks of Alzheimer's disease pathogenesis. Immunotherapies using anti-amyloid-β antibodies have been highlighted as a promising approach for the prevention and treatment of Alzheimer's disease by enhancing microglial clearance of amyloid-β peptide. However, the efficiency of antibody delivery into the brain is limited, and therefore an alternative strategy to facilitate the clearance of brain amyloid is needed.

We previously developed an artificial photo-oxygenation system using a low molecular weight catalytic compound. The photocatalyst specifically attached oxygen atoms to amyloids upon irradiation with light, and successfully reduced the neurotoxicity of aggregated amyloid-β via inhibition of amyloid formation. However, the therapeutic effect and mode of actions of the photo-oxygenation system *in vivo* remained unclear.

In this study, we demonstrate that photo-oxygenation facilitates the clearance of aggregated amyloid-β from the brains of living Alzheimer's disease model mice, and enhances the microglial degradation of amyloid-β peptide. These results suggest that photo-oxygenation may represent a novel anti-amyloid-β strategy in Alzheimer's disease, which is compatible with immunotherapy.

1 Laboratory of Neuropathology and Neuroscience, Graduate School of Pharmaceutical Sciences, University of Tokyo, Tokyo, Japan
2 Laboratory of Synthetic Organic Chemistry, Graduate School of Pharmaceutical Sciences, University of Tokyo, Tokyo, Japan
3 Laboratory of Natural Products Chemistry, Graduate School of Pharmaceutical Sciences, Nagoya University, Aichi, Japan

[‡]Present address: Department of Medicinal Chemistry, School of Pharmacy, Tokyo University of Pharmacy and Life Sciences, Tokyo, Japan

Correspondence to: Taisuke Tomita
Laboratory of Neuropathology and Neuroscience, Graduate School of Pharmaceutical Sciences
University of Tokyo, Tokyo, Japan
E-mail: taisuke@mol.f.u-tokyo.ac.jp

Correspondence may also be addressed to: Motomu Kanai
Laboratory of Synthetic Organic Chemistry, Graduate School of Pharmaceutical Sciences
University of Tokyo, Tokyo, Japan
E-mail: kanai@mol.f.u-tokyo.ac.jp

Yohei Sohma
E-mail: ysohma@mol.f.u-tokyo.ac.jp

Received June 30, 2020. Revised November 19, 2020. Accepted December 10, 2020.

Keywords: photo-oxygenation; Alzheimer's disease; amyloid-β peptide; clearance; microglia

Introduction

Alzheimer's disease is a neurodegenerative disorder characterized by the presence of two types of amyloid deposition in the brain, namely senile plaques composed of amyloid-β peptide, and neurofibrillary tangles composed of tau protein. The amyloid hypothesis, which states that the aggregation and deposition of amyloid-β initiates a cascade of neurodegenerative events, has been widely accepted.[1] Supporting this notion, several familial mutations and genetic risk factors for Alzheimer's disease have been implicated in the mechanisms underlying amyloid-β aggregation and clearance.[2,3] Therapeutic strategies have therefore focused on inhibiting amyloid-β aggregation and enhancing the clearance of amyloid-β deposits. But although several compounds that inhibit amyloid-β aggregation have been developed,[4-8] no effective treatment for Alzheimer's disease has been established to date. One reason for this is that these compounds are unable to clear existing aggregates, but instead only inhibit the formation of new ones. Moreover, amyloid PET imaging of the brains of Alzheimer's disease patients has demonstrated that amyloid-β aggregation begins before the appearance of cognitive symptoms. To prevent and/or treat Alzheimer's disease, it will therefore be necessary to target existing amyloid-β aggregates, for example by promoting their disaggregation and clearance.[9-11]

Immunotherapy using an anti-amyloid-β antibody, which opsonizes the amyloid to facilitate microglial degradation, has been highlighted as a promising approach against Alzheimer's disease. However, as the blood–brain barrier permeability of this antibody is quite limited, an alternative approach using a low molecular weight compound compatible with the immunotherapy is needed. We therefore developed an artificial photo-oxygenation system for amyloidogenic proteins using photocatalysts. These catalysts are activated by light irradiation only when they bind to a cross-β-sheet, which is a highly conserved structure in amyloids.[12-14] During relaxation, singlet oxygen is generated by the activated photocatalyst, resulting in selective oxygenation of the amyloid aggregates. We have reported previously that photo-oxygenation attenuates the aggregation of synthetic amyloid-β as well as recombinant tau, leading to lower neurotoxicity of amyloid-β *in vitro*.[12,14] In addition, the *in vivo* photo-oxygenation of Alzheimer's disease model mice using a near-infrared photoactivatable curcumin-based catalyst led to decreased amyloid-β levels in the brain.[12] These results suggest that photo-oxygenation may be a novel therapeutic strategy for Alzheimer's disease that can directly modify aggregated amyloid-β, leading to changes in the conformation and/or biochemical characteristics of the amyloid fibrils. However, the detailed mechanism whereby artificial photo-oxygenation reduces amyloid-β levels in the brain remains unknown.

In this study, we analyse the effects of *in vivo* photo-oxygenation by a BAP-1 boron-dipyrromethene (BODIPY)-based photocatalyst,[13] which has greater photo-oxygenating ability than the previous curcumin-based catalyst, in Alzheimer's disease model mice. We demonstrate that photo-oxygenation induces crosslinking of amyloid-β, and facilitates the clearance of amyloid-β deposits in the brain. Moreover, we show that we can successfully photo-oxygenate amyloid-β aggregates in the brains of patients with Alzheimer's disease, suggesting that this approach can be applied to patients with sporadic disease and thus has therapeutic potential. We then analyse the metabolism of photo-oxygenated amyloid-β aggregates, and show that photo-oxygenated aggregates are cleared faster than unmodified amyloid-β aggregates from the mouse brain, but not if the brain has been depleted of microglia. This suggests that microglia are responsible for the rapid clearance of photo-oxygenated amyloid-β. We show too that photo-oxygenated amyloid-β is localized within the lysosomes of microglial MG6 cells, and that photo-oxygenation facilitates the degradation of amyloid-β via the endolysosomal pathway. Recognition of amyloid-β, however, is unaffected. These data indicate that photo-oxygenation changes the structure and biochemical characteristics of amyloid-β fibrils, resulting in enhanced microglial clearance of deposited amyloid-β aggregates. Our results suggest that artificial photo-oxygenation may represent a novel anti-amyloid-β strategy against Alzheimer's disease that is compatible with anti-amyloid-β immunotherapy.

Materials and methods

Synthesis of the BAP-1-based photocatalyst

The BAP-1-based catalyst was synthesized as previously reported.[13] The catalyst was dissolved in dimethyl sulphoxide (DMSO) (FUJIFILM Wako Pure Chemical Corporation) to 1 mM and stored at −30°C until use.

Photo-oxygenation of synthetic preaggregated amyloid-β

Human amyloid-β1-42 solution (Peptide Institute Inc) in PBS (8 mM $Na_2HPO_412H_2O$, 2 mM $NaH_2PO_42H_2O$, 130 mM NaCl) was prepared as previously reported.[15] For the preaggregation of amyloid-β, the amyloid-β solution was incubated at 37°C for 2 h. The catalyst was then added to the preaggregated amyloid-β solution and irradiated with 660 nm light or kept in the dark at room temperature.[12,14]

MALDI-TOF mass spectrometry

For the detection of photo-oxygenated amyloid-β in Alzheimer's disease model mice, brain lysates were mixed with formic acid

(FUJIFILM Wako Pure Chemical Corporation), sonicated and lyophilized. Then, 6 M urea solution (Nacalai Tesque, Inc) was added, and the solution was purified with Ziptip® μ-C18 (Merck Millipore). The urea-soluble fraction or synthetic amyloid-β peptide solution was then mixed with 2-cyano-3-(4-hydroxyphenyl) acrylic acid (Millipore Sigma) and analysed by MALDI-TOF (matrix-assisted laser desorption/ionization-time of flight) mass spectrometry (SHIMADZU).

Amyloid-β aggregation assay and negative stain electron microscopy

For copper-mediated amyloid-β oxidation, $CuSO_4$ (25 μM; FUJIFILM Wako Pure Chemical Corporation) and H_2O_2 (250 μM; FUJIFILM Wako Pure Chemical Corporation) were added to amyloid-β and incubated for 24 h. The Thioflavin-T (ThT; Tokyo Chemical Industry Co., Ltd) assay was performed in a similar manner to that described previously.[15] Briefly, an aliquot (10 μl) of the reaction mixture [20 μM amyloid-β, preaggregated for 1 h, 0.4 μM catalyst, 10 mM phosphate buffer (7.5 mM $Na_2HPO_412H_2O$, 2.5 mM $NaH_2PO_42H_2O$)] was added to a 5 μM ThT solution (400 μl), which was freshly prepared by adding 500 μM ThT in water (4 μl) to 50 mM glycine-NaOH buffer (396 μl, pH 8.5). The fluorescence intensity of the solution (400 μl) was measured at 440 nm excitation and 480 nm emission. To visualize the amyloid-β fibrils (40 μM, preaggregated at 37°C for 2 h) with or without photo-oxygenation, negative staining and observation using electron microscopy were performed as previously reported.[13]

Cell viability assay

Cell culture and viability assays were performed in a similar manner to that described previously.[12,14] Briefly, rat pheochromocytoma PC12 cells (#CRL-1721, ATCC) suspended in 25 mM HEPES-buffered Dulbecco's modified Eagle medium (DMEM) (Thermo Fisher Scientific) containing 5% horse serum (Thermo Fisher Scientific) and 10% foetal bovine serum (Thermo Fisher Scientific) (v/v) were seeded at a density of 10 000 cells/100 μl/well on a poly-D-lysine-coated 96-well plate, and were incubated at 37°C under 5% CO_2 for 3 days. After removal of the medium, the cells were washed with 150 μl serum-free 25 mM HEPES-buffered DMEM, and incubated in 75 μl 25 mM HEPES-buffered DMEM containing 0.1% horse serum for 1 day. For the oxygenation reaction, 25 μl PBS solution containing amyloid-β preaggregated for 2 h (40 μM) and a catalyst (1.6 μM) was added to the cell culture medium (final volume: 100 μl; amyloid-β: 10 μM; catalyst: 0.4 μM), and the mixture was irradiated with a light-emitting diode (λ = 660 nm, 10 mW) at 37°C for 5 min. The cells were then incubated at 37°C under 5% CO_2 for 48 h, and the viability was determined using Cell Count Reagent SF (Nacalai Tesque, Inc), including WST-8.

Mouse experiments

All experiments using animals were performed according to the guidelines provided by the Institutional Animal Care Committee of the Graduate School of Pharmaceutical Sciences at the University of Tokyo (protocol no.: P31-11). Two Alzheimer's disease mouse models were used: $App^{NL\text{-}G\text{-}F/NL\text{-}G\text{-}F}$ mice, which are human *APP* knock-in mice with age-dependent deposition of human amyloid-β with the Arctic (E22G) mutation,[16] and APP/PS1 mice, which have no mutation in the amyloid-β sequence but which express a human *APP* gene containing the Swedish mutation K594N/M595L as well as the presenilin 1 gene with exon 9 deleted.[17] Wild-type animals were 8-week-old C57BL/6J mice (Japan SLC, Inc). All animals were maintained on a 12-h light/dark cycle with food and water available *ad libitum*.

Human brain samples

Samples of brain tissue from patients with Alzheimer's disease and aged controls were obtained from the tissue bank at the University of Pennsylvania Alzheimer's Disease Core Center (ADCC) and the Center for Neurodegenerative Disease Research (CNDR). Alzheimer's disease and control patients were diagnosed symptomatically and pathologically at ADCC-CNDR as previously described.[18] All samples used in experiments were obtained from temporal cortex under the approval of the institutional review board, ADCC-CNDR, and the institutional ethical committee of the Graduate School of Pharmaceutical Sciences, University of Tokyo (No. 2-1).

Photo-oxygenation of amyloid-β amyloid from brain lysates of Alzheimer's disease mice

The cortex and hippocampi from 7-month-old $App^{NL\text{-}G\text{-}F/NL\text{-}G\text{-}F}$ mice or 14-month-old heterozygous female APP/PS1 mice were homogenized in PBS, and lysates were stored at −80°C until use. For photo-oxygenation, the catalyst (50 μM) was added to the brain lysate and irradiated with 660 nm light or kept in the dark at room temperature.

Photo-oxygenation of amyloid-β amyloid from lysates of human brain samples

The temporal cortex from an Alzheimer's disease patient (age: 49, post-mortem interval: 16 h) and a control subject (age: 47, post-mortem interval: 12 h) were homogenized using 10 × volume of Tris-buffered saline (TBS) (50 mM Tris, 150 mM NaCl, cOmplete™ EDTA+; Millipore Sigma, pH 7.6). For photo-oxygenation, the catalyst (50 μM) was added to the brain lysate and irradiated with 660 nm light for 4 h or kept in the dark at room temperature.

Immunoblot analysis

Samples were separated by SDS-PAGE using a 15% Tris-Tricine gel with 0.1% sodium dodecyl sulphate (FUJIFILM Wako Pure Chemical Corporation) running buffer under reducing conditions (with 1% 2-mercaptoethanol; Millipore Sigma). Molecular weights were estimated using Precision Plus Protein™ Dual Color standards (Bio-Rad). Immunoblot analysis was performed using an anti-amyloid-β antibody (82E1; IBL), an anti-tyrosine dimer antibody (1C3; Japan Institute for the Control of Aging, NIKKEN SEIL. Co, Ltd) and an anti-α-tubulin antibody (DM1A; Millipore Sigma).

Photo-oxygenation in the brains of live Alzheimer's disease mice

The catalyst (50 μM, 4.5 μl) was injected into the right hippocampus [anteroposterior (AP): –2.0 mm; mediolateral (ML): –1.5 mm; dorsoventral (DV): –1.3 mm] of 7-month-old *App*$^{NL\text{-}G\text{-}F/NL\text{-}G\text{-}F}$ mice over 15 min through a guide cannula (C200GS-5/SPC, Plastics1) penetrating the skull. After injection, the right hippocampus was irradiated with 660 nm light (1.5 mW, Doric Lenses) for 30 min. The irradiation was repeated once a day for 7 days (4 days + 1 day break + 3 days). At 24 h after the final irradiation, the injected area of the right hippocampus was sampled. The left hippocampus, which was not treated with the catalyst and light, was used as a control. Both hippocampi were homogenized and stepwise fractionated. Briefly, hippocampi were homogenized using 10 × volume of TBS buffer and centrifuged (260 000*g*, 20 min, 4°C) to obtain the soluble fraction (TBS fraction), followed by extraction using 2% Triton™ X-100/TBS buffer (FUJIFILM Wako Pure Chemical Corporation). After centrifugation, precipitates were homogenized using 70% formic acid to acquire the insoluble fraction (formic acid fraction). The formic acid fraction was evaporated and dissolved in DMSO. Protein concentrations were determined using the BCA assay (TaKaRa Bio).

Clearance of photo-oxygenated amyloid-β injected into wild-type mouse brains

Preaggregated amyloid-β (40 μM, incubated at 37°C for 2 h) mixed with the catalyst (10 μM) was irradiated with 660 nm light for 30 min. Unmodified (without irradiation) and photo-oxygenated amyloid-β (10 μl each) was injected into the left (AP: –2.0 mm; ML: +1.5 mm; DV: –1.3 mm) and right hippocampi (AP: –2.0 mm; ML: –1.5 mm; DV: –1.3 mm) of 8-week-old wild-type mice (C57/BL6J) over 10 min. After 24 h, both hippocampi were sampled and stepwise fractionated to analyse amyloid-β levels using immunoblotting. For normalization, photo-oxygenated amyloid-β was mixed with wild-type mouse brain lysate, fractionated and subjected to immunoblot analysis.

Depletion of microglia by PLX3397 treatment

PLX3397[19] was synthesized as described previously[20] and formulated in AIN-76A standard chow by Research Diets Inc. The chow was given to wild-type mice (C57/BL6J) at 290 mg/kg for 21 days. Depletion of microglia was confirmed by immunohistochemistry with an anti-Iba1 antibody (019-19741; FUJIFILM Wako Pure Chemical Corporation).

Clearance of photo-oxygenated amyloid-β in brain lysates from wild-type mice

Brain lysates derived from wild-type mice were centrifuged (3000*g*, 5 min). Supernatants were mixed with either photo-oxygenated or unmodified amyloid-β fibrils, and incubated in the presence or absence of the protease inhibitor cocktail, cOmplete™ EDTA+ (Millipore Sigma), at room temperature for 24 h, and then subjected to immunoblotting to analyse amyloid-β levels.

Clearance of photo-oxygenated amyloid-β by MG6 or H4 cells

The mouse microglial cell line MG6 (RCB2403)[21,22] was obtained from RIKEN Bioresource Center (Ibaraki, Japan), and maintained in DMEM (Thermo Fisher Scientific) with 10% foetal bovine serum (Thermo Fisher Scientific), penicillin/streptomycin (Thermo Fisher Scientific), 10 μg/ml insulin (Millipore Sigma), and 0.1 mM 2-mercaptoethanol (Millipore Sigma) at 37°C and 5% CO_2. H4 cells (#HTB-148, ATCC), from a human astrocytoma cell line, were maintained in DMEM with 10% foetal bovine serum, penicillin/streptomycin at 37°C and 5% CO_2.[23]

MG6 or H4 cells were seeded onto 24-well plates (10^5 cells per well) and incubated overnight. For the analysis of amyloid-β uptake by MG6 cells, cells were treated with photo-oxygenated or unmodified amyloid-β (500 nM each), and incubated for 24 h. For the analysis of amyloid-β degradation in MG6 or H4 cells, cells were pretreated with amyloid-β (500 nM each) for 1 h followed by washing out of the media and further incubation with/without 50 μM leupeptin (Millipore Sigma). Cells were collected and the amounts of amyloid-β within the cells were analysed by immunoblotting.

Immunocytochemistry of photo-oxygenated amyloid-β

For preparation of HiLyte™ Fluor 488-labelled aggregated amyloid-β, unlabelled amyloid-β1-42 was mixed with HiLyte™ Fluor 488-labelled Aβ1-42 (AnaSpec) at a 20:1 ratio before aggregation. Two hours after incubation for pre-aggregation, the mixed aggregates were photo-oxygenated. MG6 cells were plated at 2.0×10^5 cells/well onto glass coverslips in 6-well plates (Sumitomo Bakelite) and cultured overnight. Cells were treated with 500 nM HiLyte™ Fluor 488-labelled photo-oxygenated amyloid-β for 1 h. After washing out of medium, cells were incubated for a further 3 h and fixed with 4% paraformaldehyde/PBS (FUJIFILM Wako Pure Chemical Corporation). After washing three times with PBS, permeabilization with 0.1% Triton™ X-100/PBS for 5 min, and blocking with 10% normal donkey serum for 30 min, cells were stained with anti-CD68 rat monoclonal antibody (1:100, Bio-Rad) in PBS for 1 h. After incubation with Alexa Fluor® 546 conjugated anti-rat IgG (1:500, Thermo Fisher Scientific), cells were mounted with ProLong™ Diamond (Thermo Fisher Scientific). Images were acquired with super-resolution microscopy (ZEISS LSM980 with Airyscan 2).

Amyloid-β measurement using ELISA

To measure amyloid-β in insoluble formic acid fractions, samples of wild-type mouse brains were injected with photo-oxygenated amyloid-β and diluted appropriately; amyloid-β levels were then analysed using the Human/Rat β Amyloid(42) ELISA Kit, High Sensitivity (292-64501, FUJIFILM Wako Pure Chemical Corporation) as previously described.[24]

Statistical analysis

Data are presented as mean ± standard error of the mean (SEM) or mean ± standard deviation (SD). Samples were compared using a two-tailed Student *t*-test, Welch *t*-test, or ANOVA followed by the Tukey *post hoc* test. A *P*-value of <0.05 was considered statistically significant. KyPlot (KyensLab Inc.) was used to perform the statistical analysis.

Data availability

The raw data that support the findings of this study are available from the corresponding author on reasonable request.

Results

Photo-oxygenation using a BAP-1-based photocatalyst reduced amyloid-β aggregation potency and neurotoxicity

BAP-1 is a BODIPY-based imaging probe for amyloid-β aggregates *in vitro* and *in vivo*.[25] We developed a BAP-1-based photocatalyst,[13] with greater photo-oxygenation ability for tau and amyloid than the previous curcumin-based catalyst (Fig. 1A). However, the potency of this catalyst for amyloid-β remains unclear. We have previously shown that photo-oxygenation by ThT-based as well as curcumin-based photocatalysts inhibited the aggregation and cellular toxicity of amyloid-β.[12,14] As expected, the BAP-1-based catalyst was also able to photo-oxygenate preformed synthetic amyloid-β fibrils upon irradiation at 660 nm near-infrared (Supplementary Fig. 1A and B). In the amyloid-β fibrillization assay using ThT, the irradiation of synthetic amyloid-β coincubated with the catalyst substantially lowered the ThT intensity, indicating that photo-oxygenation inhibits the fibrillization of synthetic amyloid-β (Supplementary Fig. 1C, column D versus columns A–C). Moreover, the neurotoxicity of photo-oxygenated amyloid-β fibrils in PC12 cells—a cell line derived from rat pheochromocytoma—was significantly lower than that of unmodified amyloid-β fibrils (Supplementary Fig. 1D: column H versus columns C, D and G). These data suggest that photo-oxygenation of amyloid-β aggregates by the BAP-1-based photocatalyst reduces amyloid-β aggregation and toxicity, by interfering with toxic amyloid formation.

Photo-oxygenation changes the structural and/or biochemical characteristics of amyloid-β amyloid

As photo-oxygenation covalently incorporates oxygen atoms into amyloid-β aggregates, we hypothesized that photo-oxygenation may alter the conformation and/or biochemical characteristics of the amyloid fibrils. To investigate this possibility, we analysed photo-oxygenated synthetic amyloid-β fibrils by SDS-PAGE and immunoblot (Fig. 1B). Aggregated amyloid-β that had been dissociated by SDS was mainly observed as 5 kDa amyloid-β monomers. In addition, a 10 kDa amyloid-β dimer band as well as a smear were detected with an anti-amyloid-β antibody (Fig. 1C, vehicle and catalyst lanes). Upon photo-oxygenation, the intensity of the amyloid-β smear increased and some extra bands with higher molecular weights appeared (Fig. 1C, catalyst + light lane), suggesting that the conformation of the amyloid-β fibrils was altered both structurally and biochemically by the photo-oxygenation. Notably, a 10 kDa amyloid-β band, which showed a slightly lower mobility than that of the 10 kDa amyloid-β dimer in the unmodified amyloid-β aggregates, was detected in the photo-oxygenated amyloid fibrils. We defined this band as 10 kDa oxy-amyloid-β, which was specifically generated by the photo-oxygenation. To test whether this 10 kDa oxy-amyloid-β species represents a crosslinked product via the 10th Tyr residue in the amyloid-β sequence, as previously observed after oxidation using copper and H_2O_2,[26] we analysed the photo-oxygenated amyloid-β using an anti-Tyr dimer-specific antibody. However, this antibody did not detect any amyloid-β in the photo-oxygenated amyloid-β fibrils (Fig. 1D), indicating that the 10 kDa oxy-amyloid-β and amyloid-β oligomers produced by photo-oxygenation were different from the oxidized Tyr-mediated amyloid-β dimers. Finally, oxygenated amyloid-β species as well as the 10 kDa oxy-amyloid-β band were also found in the photo-oxygenated amyloid-β amyloid fibrils derived from the brains of two types of Alzheimer's disease model mice, $App^{NL\text{-}G\text{-}F/NL\text{-}G\text{-}F}$,[16] and APP/PS1,[17] by both MALDI-TOF mass spectrometry and immunoblot analyses (Fig. 1E, F and Supplementary Fig. 2). Only 5 kDa and 10 kDa amyloid-β bands were observed in photo-oxygenated brain lysates of $App^{NL\text{-}G\text{-}F/NL\text{-}G\text{-}F}$ and APP/PS1 mice, and the larger aggregates were not changed by photo-oxygenation (Supplementary Fig. 2). These data suggest that aggregated amyloid-β was also photo-oxygenated in the brains of Alzheimer's disease model mice, and that the 10 kDa oxy-amyloid-β species was an indicator of successful photo-oxygenation. Furthermore, increased intensity of the amyloid-β band around 10 kDa was also seen following photo-oxygenation of amyloid-β derived from the brains of Alzheimer's disease patients (Fig. 1G), reflecting the appearance of the 10 kDa oxy-amyloid-β species. This suggests that photo-oxygenation could be used to target amyloid-β deposits in the brains of patients with sporadic Alzheimer's disease.

Photo-oxygenation reduces brain amyloid-β levels

To demonstrate the catalytic photo-oxygenation of amyloid-β aggregates in living mouse brains, 7-month-old $App^{NL\text{-}G\text{-}F/NL\text{-}G\text{-}F}$ mice were injected in the right hippocampal region with the catalyst accompanied by light irradiation (Fig. 2A). Injection and irradiation were performed once a day for 7

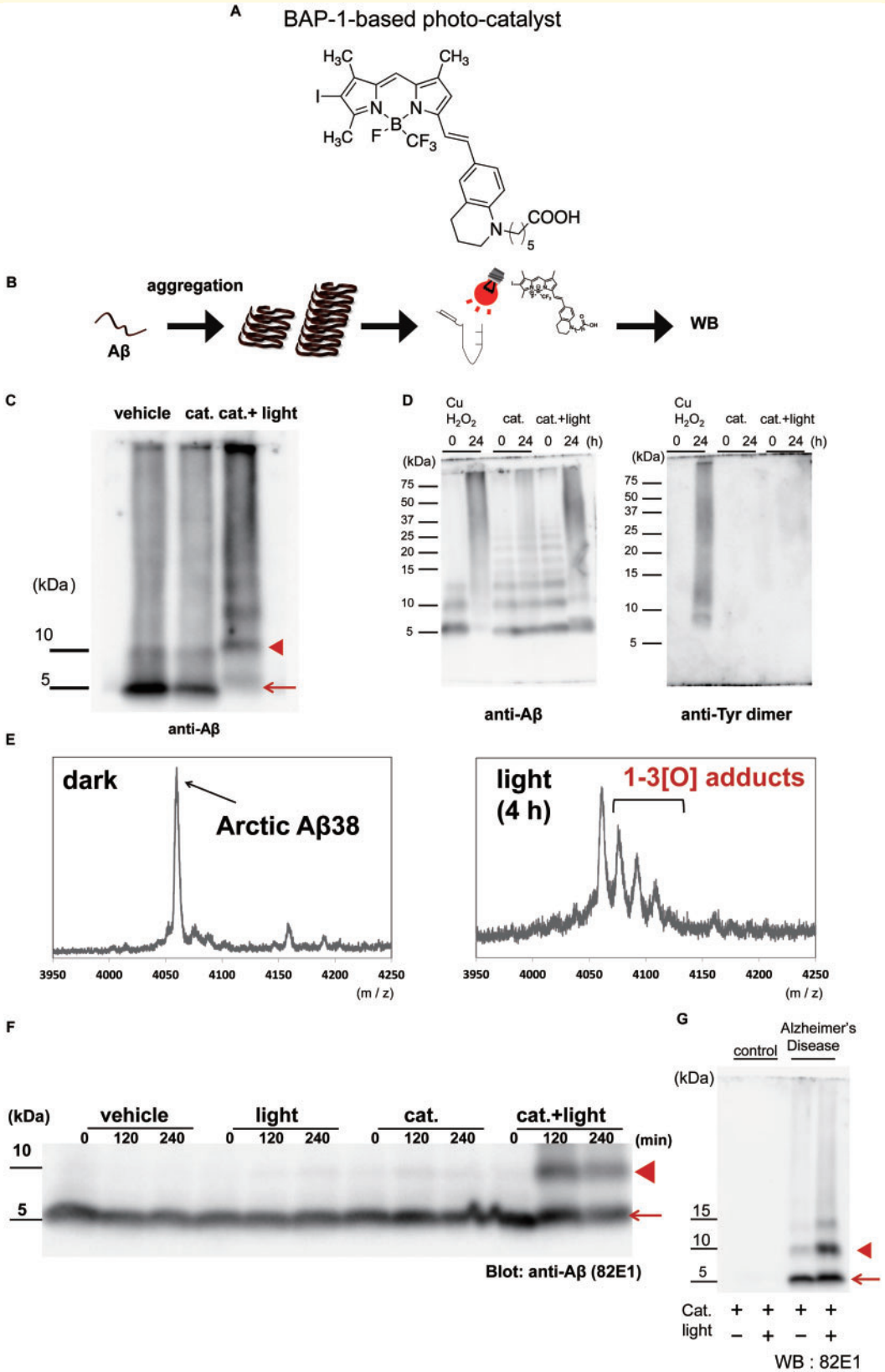

Figure 1 Photo-oxygenation shifts the mobility of amyloid-β on immunoblotting. (**A**) Structure of the photocatalyst. (**B**) Photo-oxygenation protocol. Preaggregated amyloid-β (Aβ) was mixed with the catalyst and irradiated with 660 nm light for 5 min, followed by immunoblot analysis. (**C**) Immunoblot analysis of amyloid-β aggregates with or without photo-oxygenation. Vehicle = no catalyst (without photo-oxygenation); cat. = catalyst only (without photo-oxygenation); cat. + light = catalyst and light irradiation (photo-oxygenation). (**D**) Immunoblot analysis. Photo-oxygenated amyloid-β and copper-mediated oxidized amyloid-β were subjected to immunoblot analysis using an

(continued)

days, and both the left and right hippocampi were extracted 24 h after the final treatment, to analyse levels of soluble and insoluble amyloid-β. The 10 kDa oxy-amyloid-β species was specifically detected in the insoluble fraction of right hippocampal lysates after the photo-oxygenation reaction, indicating that the deposited amyloid-β was successfully photo-oxygenated in the living mouse brain (Fig. 2B, arrowhead in the rightmost lane), although levels of the 10 kDa oxy-amyloid-β species were relatively low. Moreover, photo-oxygenation substantially reduced levels of monomeric amyloid-β in both the soluble and insoluble fractions (Fig. 2B and C). Taken together, these data suggest that photo-oxygenation promotes the clearance of soluble and insoluble amyloid-β aggregates, including oligomers and fibrils *in vivo*, in addition to inhibiting amyloid-β formation.

Photo-oxygenated amyloid-β is rapidly cleared independent of fibril dissociation and proteolytic degradation

We next investigated the mechanism underlying the rapid clearance of photo-oxygenated amyloid-β aggregates *in vivo*. Photo-oxygenated and unmodified amyloid-β aggregates were injected into the right and left hippocampi, respectively, of wild-type mouse brains, and the levels of amyloid-β remaining in the hippocampi 24 h after injection were analysed (Fig. 3A). Immunoblot analysis demonstrated that levels of both the 5 kDa and 10 kDa amyloid-β species in both the soluble and insoluble fractions of photo-oxygenated amyloid-β fibrils were significantly lower than the levels of these species in unmodified amyloid-β aggregates (Fig. 3B–E); the levels were consistent with the amount of amyloid-β remaining in the insoluble fraction as revealed by ELISA (Supplementary Fig. 3). In particular, a reduction in photo-oxygenated amyloid-β levels in the insoluble fraction suggests that large amyloid-β aggregates were cleared by a single photo-oxygenation. In addition, the level of the 10 kDa oxy-amyloid-β species was also reduced faster than that of the native amyloid-β dimer, suggesting that 10 kDa oxy-amyloid-β has different properties to the dimeric species composed of unmodified amyloid-β.

We recently reported that photo-oxygenation induces the rupture of heat-denatured β-lactoglobulin and α-synuclein fibrils.[27] To investigate the possibility that photo-oxygenation also induces rupture of amyloid-β fibrils, the structure of photo-oxygenated amyloid-β aggregates was examined using electron microscopy (Supplementary Fig. 4A). However, neither the size nor the length of aggregated amyloid-β was altered by photo-oxygenation, indicating that the dissociation of aggregated amyloid-β is not a major pathway for the rapid clearance of photo-oxygenated amyloid-β. Another possible mechanism for the clearance of photo-oxygenated amyloid-β in the brain is enhanced proteolytic degradation. To test this possibility, photo-oxygenated amyloid-β was mixed with brain lysates from wild-type mice and incubated for 24 h (Supplementary Fig. 4B). The 5 kDa amyloid-β species in the soluble fraction disappeared after the incubation, irrespective of the photo-oxygenation, whereas the dimeric and oligomeric amyloid-β species remained (Supplementary Fig. 4C). The 5 kDa amyloid-β species remained in the soluble fraction upon coincubation with a protease inhibitor cocktail, indicating that the 5 kDa amyloid-β species was proteolytically degraded in the brain. However, no significant difference was observed in the degradation rate between unmodified and photo-oxygenated amyloid-β. In addition, neither photo-oxygenated nor unmodified amyloid-β aggregates were degraded in the insoluble fraction, suggesting that proteases in the brain lysate at neutral pH are not responsible for the enhanced clearance of photo-oxygenated amyloid-β amyloid in live mice.

Depletion of microglia inhibits the rapid clearance of photo-oxygenated amyloid-β

Next, we focused on the role of microglia in the clearance of photo-oxygenated amyloid-β. Microglia can phagocytose amyloid-β and degrade it via the endolysosomal pathway, and microglial dysfunction has been implicated in the pathogenesis of Alzheimer's disease.[3,28-30] To investigate whether microglia are responsible for the rapid clearance of photo-oxygenated amyloid-β, we treated with pexidartinib (PLX3397), a colony stimulating factor 1 receptor inhibitor that has been used to deplete mouse brain microglia.[19] Immunostaining confirmed that 21 days of treatment with PLX3397 successfully depleted microglia (Fig. 4A). Photo-oxygenated and unmodified amyloid-β aggregates were then injected into the right and left hippocampi, respectively, of wild-type mouse brains with or without treatment with PLX3397 (Fig. 4B). Immunoblot analysis of amyloid-β

Figure 1 Continued
anti-amyloid-β antibody (82E1, *left*) and an anti-Tyr dimer-specific antibody (*right*). (**E**) MALDI-TOF mass spectrometry analysis of photo-oxygenation in brain lysates. Brain lysates were prepared from 7-month-old $App^{NL\text{-}G\text{-}F/NL\text{-}G\text{-}F}$ mice. The catalyst was mixed with the lysates and irradiated with 660 nm light for 4 h, followed by MALDI-TOF mass spectrometry analysis. Additional peaks corresponding to 1–3[O] adducts appeared upon photo-oxygenation. (**F**) Immunoblot analysis of photo-oxygenation of the brain lysate in **E**. (**G**) Immunoblot analysis of photo-oxygenation of the brain lysate derived from a control or an Alzheimer's disease patient, using an anti-amyloid-β antibody (82E1). In **C**, **F** and **G**: arrow = amyloid-β; arrowhead = 10 kDa oxy-amyloid-β. WB = western blot.

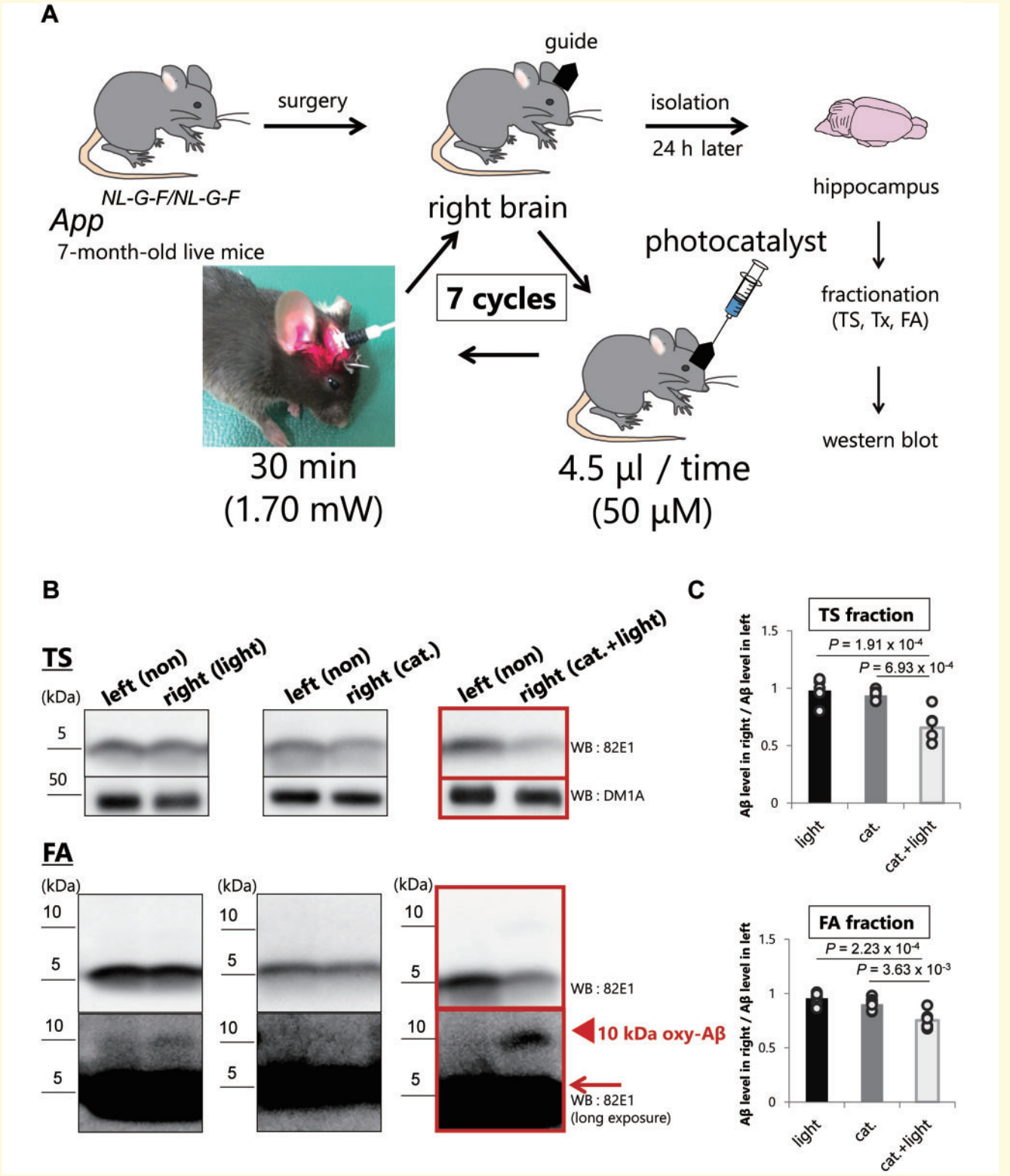

Figure 2 Photo-oxygenation reduces amyloid-β levels in the brains of Alzheimer's disease mouse models. (**A**) Method of photo-oxygenation in live 7-month-old *App*$^{NL\text{-}G\text{-}F/NL\text{-}G\text{-}F}$ mice. FA = formic acid fraction (insoluble fraction); TS = Tris-buffered saline fraction (TS; soluble fraction); Tx = Triton X-100 soluble fraction. (**B**) Representative immunoblot results for the hippocampi of mice subjected to each condition, using an anti-amyloid-β antibody (82E1) and an anti-α-tubulin antibody (DM1A) as loading control. The *bottom* panel in the formic acid fraction shows a long exposure of the upper immunoblot. Light = light irradiation only; cat. = catalyst injection only; cat. + light = catalyst injection and light irradiation (photo-oxygenation); arrow = amyloid-β; arrowhead = 10 kDa oxy-amyloid-β. (**C**) The ratio of relative amyloid-β levels in the right/left hippocampi. Light only = 1.0; *n* = 6; *P*-values from a Tukey test are shown. WB = western blot.

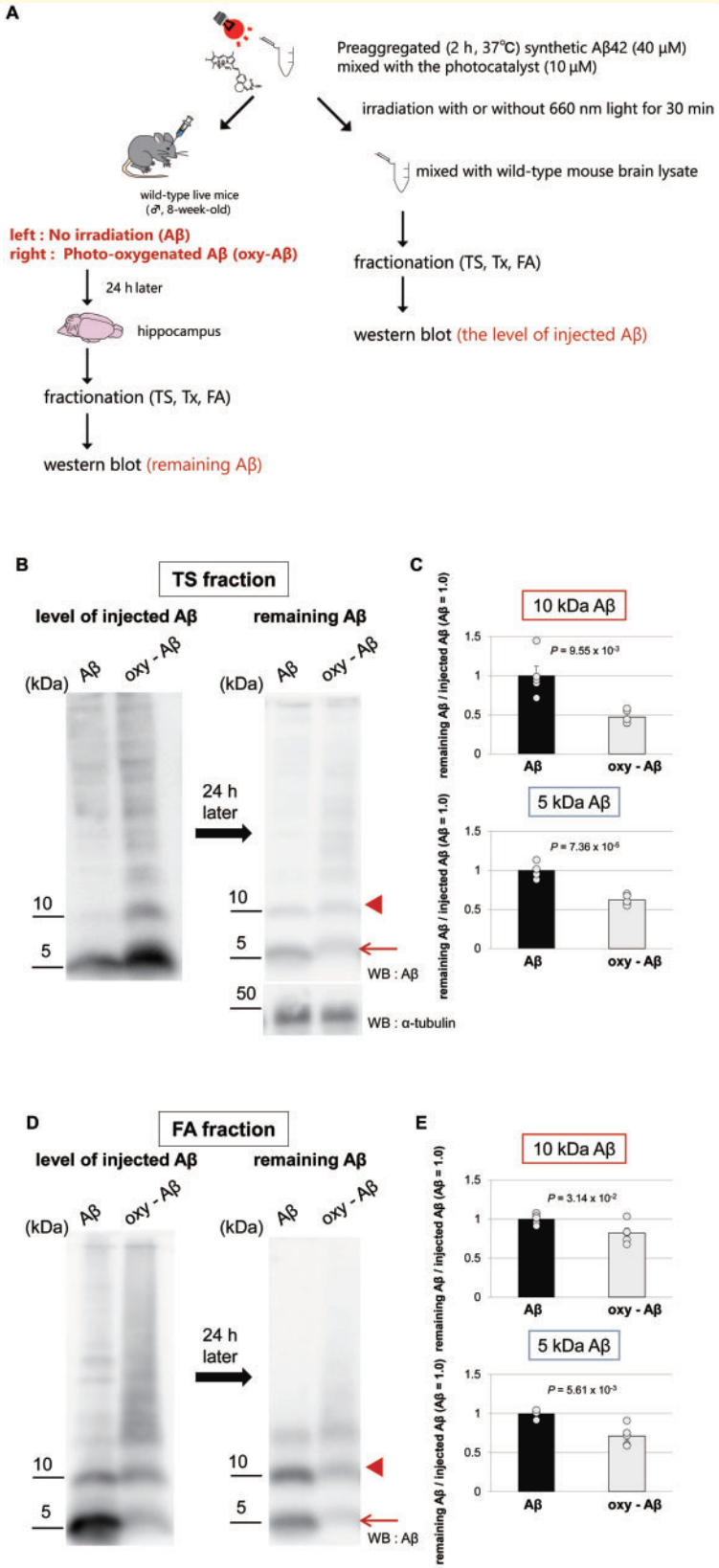

Figure 3 Photo-oxygenated amyloid-β is rapidly cleared from the brain. (**A**) Protocol for the injection of photo-oxygenated amyloid-β into wild-type mouse brains. (**B** and **D**) Representative immunoblot of the Tris-buffered saline (TS) fraction (**B**) and formic acid fraction (FA) (**D**) before (level of injected amyloid-β) and 24 h after injection (remaining amyloid-β) using an anti-amyloid-β antibody (82E1) and an anti-α-tubulin antibody (DM1A). Arrow = amyloid-β; arrowhead = 10 kDa oxy-amyloid-β. (**C** and **E**) Ratios of remaining amyloid-β to injected amyloid-β in **B** and **D**, respectively (n = 5, P-values calculated by the Student t-test). WB = western blot.

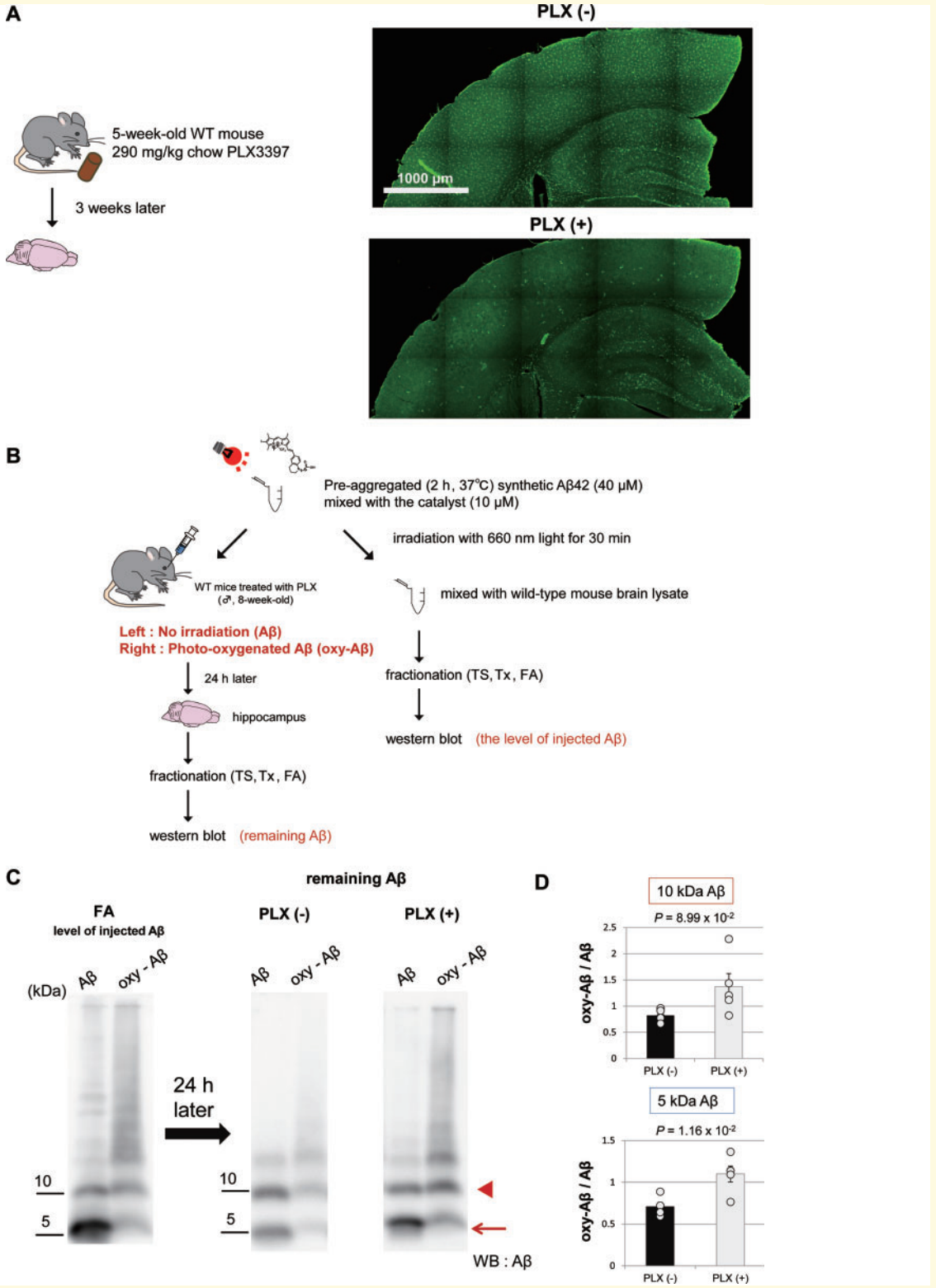

Figure 4 Depleting microglia inhibits the rapid clearance of photo-oxygenated amyloid-β. (**A**) Depletion of microglia from the brains of wild-type (WT) mice by treatment with PLX3397. Five-week-old wild-type mice were treated with PLX3397 in chow for 21 days, and the brains were analysed immunohistochemically with an anti-Iba1 antibody. Scale bar = 1 mm. (**B**) Protocol for the injection of photo-oxygenated amyloid-β into the brains of wild-type mice with or without treatment with PLX3397. (**C**) Representative immunoblot of the formic acid fraction before (level of injected amyloid-β) and 24 h after injection [remaining amyloid-β, in PLX (-) and PLX (+) mouse brain] using an anti-amyloid-β antibody (82E1). Arrow = amyloid-β; arrowhead = 10 kDa oxy-amyloid-β. (**D**) Ratios of remaining photo-oxygenated amyloid-β to unmodified amyloid-β in **C** ($n = 5$, *P*-values calculated by Welch's *t*-test). FA = formic acid fraction (insoluble fraction); TS = Tris-buffered saline fraction (TS; soluble fraction); Tx = Triton X-100 soluble fraction.

remaining 24 h after injection demonstrated that the ratio of photo-oxygenated amyloid-β to unmodified amyloid-β in the formic acid fraction was substantially increased by treatment with PLX3397 (Fig. 4C and D), indicating that the depletion of microglia inhibits the rapid degradation of photo-oxygenated amyloid-β aggregates. These data thus suggest that microglia are responsible for the rapid clearance of photo-oxygenated amyloid-β.

Photo-oxygenated amyloid-β is rapidly degraded via endolysosomes in MG6 cells

To clarify the role of microglial activity in facilitating the clearance of photo-oxygenated amyloid-β, we performed an amyloid-β uptake assay using the MG6 mouse microglial cell line.[21,22] Photo-oxygenated and unmodified amyloid-β aggregates were added to the culture media, and incubated for the times indicated (Fig. 5A). No significant difference was observed in the rate of uptake of photo-oxygenated versus unmodified amyloid-β fibrils (Fig. 5B and C), suggesting that photo-oxygenation does not affect the mechanism by which amyloid-β is recognized in MG6 cells. Since immunocytochemistry showed that photo-oxygenated amyloid-β was localized in CD68-positive lysosomes within MG6 cells (Supplementary Fig. 5), we next assessed the rate of degradation of amyloid-β in MG6 cells by analysing additional incubation periods after the washout of amyloid-β in conditioned medium (Fig. 5D). At almost all time points, the levels of photo-oxygenated amyloid-β remaining in MG6 lysates were significantly lower than the levels of unmodified amyloid-β aggregates, indicating that photo-oxygenated amyloid-β was degraded faster than unmodified amyloid-β within MG6 cells (Fig. 5E and F). In addition, this rapid clearance of photo-oxygenated amyloid-β was completely abolished by treatment with leupeptin (Fig. 5G–I), a lysosomal serine/cysteine protease inhibitor.[31] Notably, this rapid clearance of photo-oxygenated amyloid-β was not observed in the H4 human astrocytoma cell line (Supplementary Fig. 6). Taken together, these data suggest that photo-oxygenated amyloid-β is rapidly degraded in the brain by the lysosomal system within microglia, but not astrocytes.

Discussion

We have previously shown that photo-oxygenation inhibits amyloid fibril formation *in vitro* and amyloid-β toxicity in cultured cells. In this study, we demonstrate that our photo-oxygenation approach using the BAP-1-based photocatalyst with light irradiation promotes the clearance of insoluble amyloid-β species from living mouse brains. In addition, we show that this photo-oxygenation can be applied to amyloid-β deposits in the brains of patients with sporadic Alzheimer's disease. We also reveal the underlying mechanism by showing that microglia are responsible for the rapid clearance of photo-oxygenated amyloid-β aggregates, and that photo-oxygenation facilitates the intracellular degradation of amyloid-β aggregates via the endolysosomal pathway in microglial MG6 cells. This suggests that the enhanced clearance of photo-oxygenated amyloid-β in the mouse brain occurs as a result of increased microglial intracellular degradation.

We have previously demonstrated that, in addition to methionine and tyrosine residues, our photo-oxygenation system also covalently incorporates oxygen atoms into histidine residues of the amyloid-β sequence.[12,14] The generation of oxygenated histidine (i.e. 2-oxo-histidine and its ring-ruptured products) is a unique mechanism of singlet oxygen-mediated amino acid oxidation, which is similar to our photo-oxygenation using photocatalysts.[32-34] In general, oxygenated histidine induces crosslinking, inactivation and constitutional changes in proteins.[32] Consistent with this, photo-oxygenation resulted in the appearance of 10 kDa oxy-amyloid-β as well as multiple crosslinked amyloid-β peptides, which were not recognized by the anti-tyrosine dimer antibody. Thus, histidine oxygenation and crosslinking may cause structural changes in the amyloid fibrils, although substantial changes in their morphology were not evident. Indeed, we recently reported that histidine residues are necessary for the rupturing of α-synuclein fibrils, which was induced by a photocatalyst.[27] Thus, the generation of oxygenated histidine-containing amyloid-β fibrils might destabilize the amyloid conformation.

Several studies have indicated that microglia phagocytose and subsequently degrade amyloid-β via the endolysosomal system. Several lysosomal proteases, such as cathepsin B, have been implicated in this amyloid-β degradation.[35] Moreover, a recent study demonstrated that tripeptidyl peptidase 1 (TPP1), which is a lysosomal serine protease, destabilizes amyloid-β fibrils via multiple endoproteolytic cleavages within the β-sheet domain.[36] Thus, photo-oxygenation accompanied by structural changes promotes the degradation of amyloid-β in the endolysosomal pathway, for example, by facilitating cleavage by lysosomal degrading enzymes, such as TPP1 (Fig. 6). This notion is further supported by our results showing that brain proteases working at neutral pH were not associated with the degradation of amyloid-β aggregates; the rapid clearance of photo-oxygenated amyloid-β was completely abolished by treatment with the lysosomal serine/cysteine protease inhibitor leupeptin; and photo-oxygenated amyloid-β was localized to the lysosomes of microglial MG6 cells. Moreover, extensive biochemical analyses of patient-derived senile plaques demonstrated the presence of oxidized methionine residues in the deposited amyloid-β.[37] However, oxygenated histidine has not been reported, suggesting that oxygenated histidine may facilitate amyloid-β degradation/clearance in the human brain. Nevertheless, we are unable to exclude the possibility that photo-oxygenated amyloid-β was rapidly cleared through other pathways, such as efflux transport across the blood–brain barrier,[38] the glymphatic/lymphatic systems,[39]

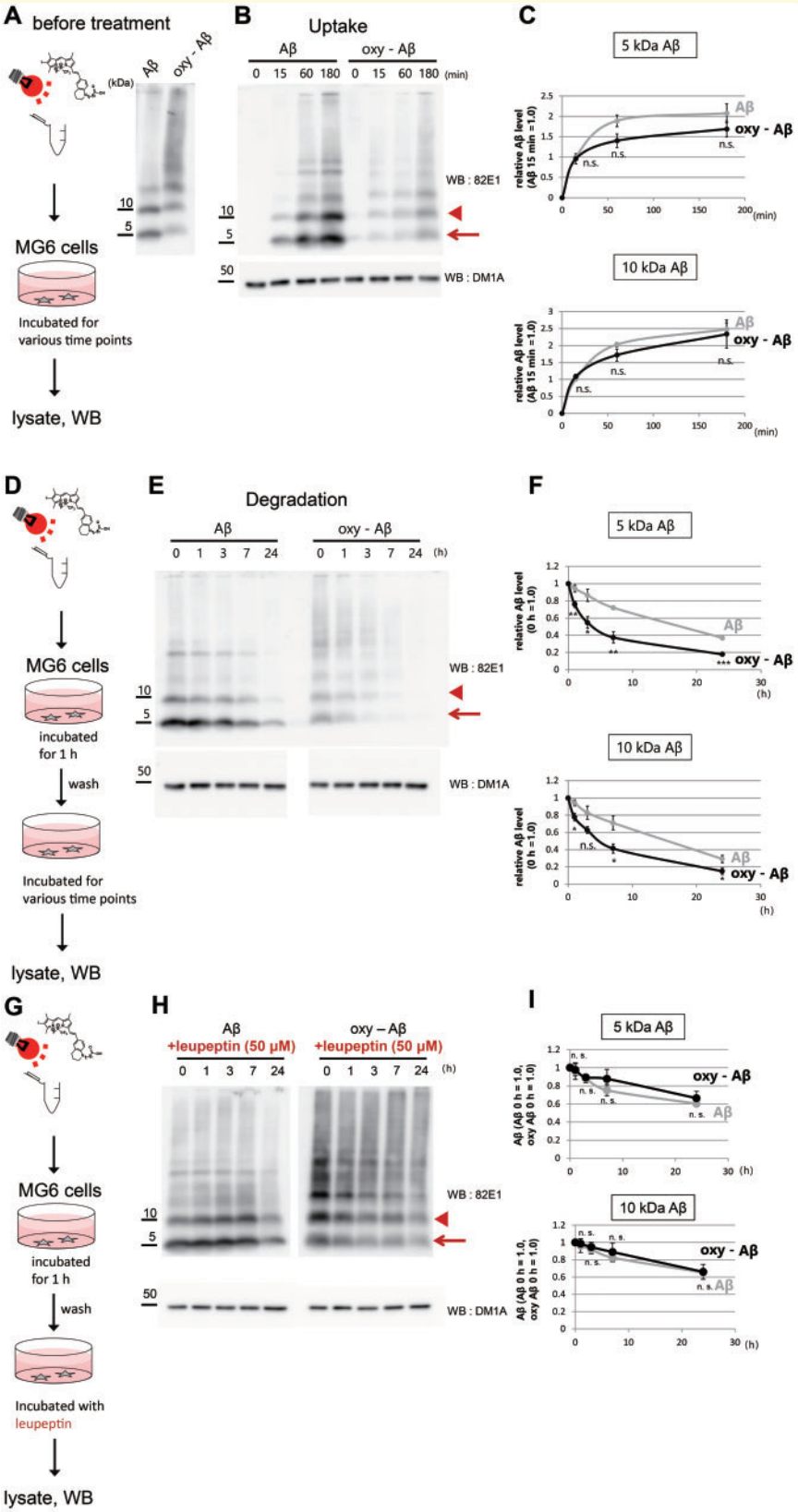

Figure 5 Photo-oxygenated amyloid-β is degraded faster than unmodified amyloid-β in MG6 cells. (**A**) Schematic depiction of the amyloid-β uptake assay. Immunoblot analysis of treated photo-oxygenated amyloid-β (oxy-Aβ) and unmodified amyloid-β fibrils (Aβ) is shown. (**B**) Representative immunoblot of amyloid-β-treated MG6 cell lysates using an anti-amyloid-β antibody (82E1) and an anti-α-tubulin antibody (DM1A). (**C**) Quantitative analyses of relative amyloid-β levels in the MG6 cell lysates in **B**. Each amyloid-β level was standardized to the average incorporated amyloid-β level at 15 min incubation. Black line = oxy-amyloid-β; grey line = amyloid-β. Data were analysed by the Welch *t*-test

(continued)

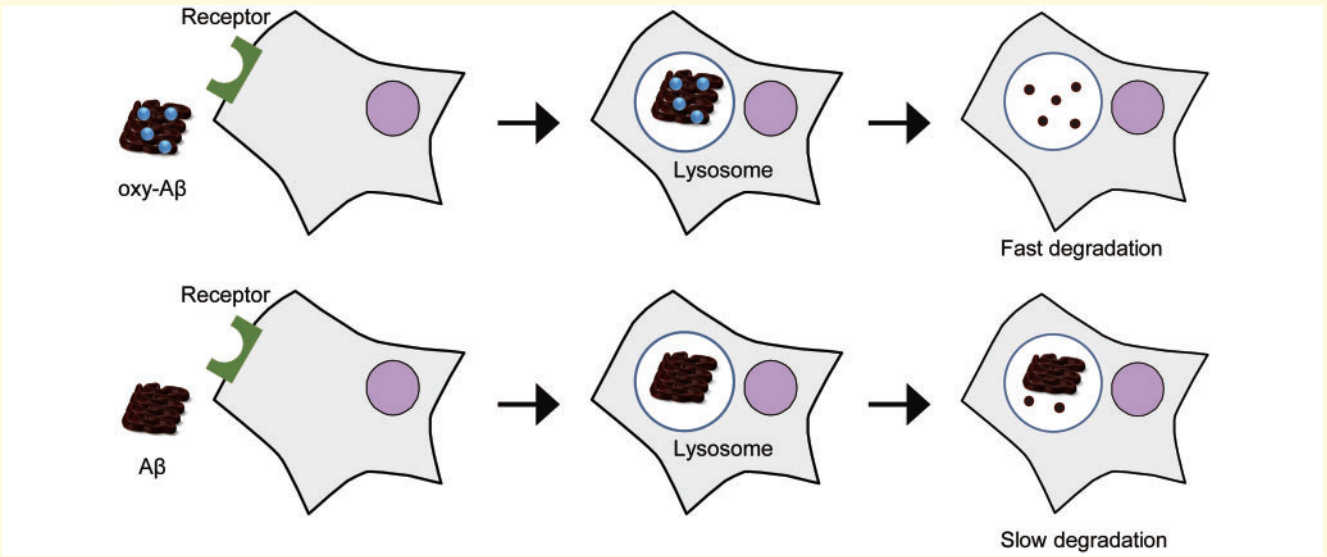

Figure 6 Mechanism of photo-oxygenation-mediated amyloid-β clearance. Both unmodified as well as photo-oxygenated amyloid-β (oxy-Aβ) fibrils are phagocytosed by microglial cells. Photo-oxygenated amyloid-β is relatively unstable and is rapidly degraded by the endolysosomal system.

and degradation by extracellular amyloid-β-degrading enzymes.[40,41] Notably, recent technological advances have led to the identification of endogenous peptides containing 2-oxo-histidine within normal tissues.[42] Moreover, histidine oxygenation of the peroxide operon regulator protein is used as a redox-sensing mechanism in *Bacillus subtilis*.[43] These findings suggest that oxygenated histidine plays physiological role(s) in protein metabolism and/or redox signalling in living organisms. Nevertheless, we plan to elucidate the molecular pathway involved in the enhanced clearance of photo-oxygenated amyloid-β *in vivo*.

Conclusion

Consistent with the amyloid hypothesis, which states that the aggregation and deposition of amyloid-β gives rise to Alzheimer's disease, our study indicates that photo-oxygenation of amyloid-β is a potential therapeutic strategy for Alzheimer's disease, and that further refinement of this approach is warranted. In support of this idea, we show that amyloid-β deposits in the brains of patients with Alzheimer's disease can also be photo-oxygenated. In addition, we have recently developed a non-invasive photo-oxygenation system using a new blood–brain barrier-permeable catalyst and irradiation with light from outside the skull without any surgery, and have shown that this approach reduces amyloid-β levels in the brain.[44] The anti-amyloid-β antibody aducanumab was recently shown to reduce the clinical decline of patients with early Alzheimer's disease, by reducing levels of amyloid-β plaques in the brain,[10] strongly suggesting that the clearance of amyloid-β aggregates from the brain is a promising approach against Alzheimer's disease. Our photo-oxygenation system using a low molecular weight catalyst may thus represent an alternative method for anti-amyloid-β therapy that is compatible with immunotherapy. Moreover, this catalyst also photo-oxygenated tau amyloid—another hallmark amyloid of Alzheimer's disease—and reduced its aggregation propensity.[13] Given that the coexistence of amyloid-β and tau amyloid is linked to cognitive decline in

Figure 5 Continued

($n = 5$). n.s. = no significant difference between the two groups. (**D**) Schematic depiction of the degradation assay. (**E**) Representative immunoblot of MG6 cells after washout of treated amyloid-β, using an anti-amyloid-β antibody (82E1) and an anti-α-tubulin antibody (DM1A). (**F**) Quantitative analyses of relative remaining amyloid-β levels in the MG6 cells in **E**. Each amyloid-β level was standardized to the average amyloid-β level with no additional incubation. Black line: oxy-amyloid-β; grey line: amyloid-β. *$P < 0.05$; **$P < 0.01$; ***$P < 0.001$ by the Welch *t*-test ($n = 5$). (**G**) Schematic depiction of the degradation assay with leupeptin. (**H**) Representative immunoblot of MG6 cells after washout of treated amyloid-β and additional incubation with leupeptin, using an anti-amyloid-β antibody (82E1) and an anti-α-tubulin antibody (DM1A). (**I**) Quantitative analyses of relative remaining amyloid-β levels in the MG6 cells in **H**. Each amyloid-β level was standardized to the average amyloid-β level with no additional incubation. Black line = oxy-amyloid-β; grey line = amyloid-β. n.s. = no significant difference between the two groups by the Welch *t*-test ($n = 3$). In **B**, **E** and **H**: arrow = amyloid-β; arrowhead = 10 kDa oxy-amyloid-β. WB = western blot.

Alzheimer's disease,[45] photo-oxygenation can be expected to be a useful strategy against Alzheimer's disease, by simultaneously reducing the toxicity of both amyloid-β and tau.

Acknowledgements

The authors wish to thank Drs T. C. Saido (Riken Center for Brain Science), T. Saito (Nagoya City University), T. Iwatsubo (Tokyo University), J. Q. Trojanowski (University of Pennsylvania) and V. M. Y. Lee (University of Pennsylvania) for valuable reagents, materials and unpublished information. The authors are also grateful to our present and previous laboratory members for helpful discussions, and Ms Shuning Liu (student in UTokyo Amgen Scholar Program 2018) for initial experiments. We also thank the patients and their families for brain donation.

Funding

This work was supported in part by a Grant-in-Aid for Scientific Research (C) (18K06653 to Y.H.), Grant-in-Aid for Young Scientists (A) (16H06216 to Y.S.), and Grant-in-Aid for Challenging Exploratory Research (19K22484 to Y.S.), and a Grant-in-Aid for Scientific Research (A) (15H02492 to T.T., 19H01015 to T.T., 20H00489 to M.K.) from the Japan Society for the Promotion of Science (JSPS), grants from Innovative Research Group by the Strategic International Brain Science Research Promotion Program (Brain/MINDS Beyond) (JP19dm0307030 to Y.H.) and Strategic International Collaborative Research Program (SICORP) (JP19jm0210058 to Y.S.), from the Japan Agency for Medical Research and Development (AMED), and a grant from Terumo Life Science Foundation (to Y.S.). S.O. is a research fellow of the JSPS.

Competing interests

The authors report no competing interests.

Supplementary material

Supplementary material is available at *Brain* online.

References

1. Selkoe DJ, Hardy J. The amyloid hypothesis of Alzheimer's disease at 25 years. *EMBO Mol Med*. 2016;8:595-608.
2. Kanekiyo T, Xu H, Bu G. ApoE and Aβ in Alzheimer's disease: accidental encounters or partners? *Neuron*. 2014;81:740-754.
3. Takatori S, Wang W, Iguchi A, Tomita T. Genetic risk factors for alzheimer disease: emerging roles of microglia in disease pathomechanisms. *Adv Exp Med Biol*. 2019;1118:83-116.
4. Baum L, Lam CWK, Cheung SK-K, et al. Six-month randomized, placebo-controlled, double-blind, pilot clinical trial of curcumin in patients with Alzheimer's disease. *J Clin Psychopharmacol*. 2008;28:110-113.
5. Frautschy SA, Hu W, Kim P, et al. Phenolic anti-inflammatory antioxidant reversal of Aβ-induced cognitive deficits and neuropathology. *Neurobiol Aging*. 2001;22:993-1005.
6. Hori Y, Takeda S, Cho H, et al. A Food and Drug Administration-approved asthma therapeutic agent impacts amyloid β in the brain in a transgenic model of Alzheimer disease. *J Biol Chem*. 2015;290:1966-1978.
7. Lim GP, Chu T, Yang F, Beech W, Frautschy S. A, Cole GM. The curry spice curcumin reduces oxidative damage and amyloid pathology in an Alzheimer transgenic mouse. *J Neurosci*. 2001;21:8370-8377.
8. Wang J, Ho L, Zhao W, et al. Grape-derived polyphenolics prevent a oligomerization and attenuate cognitive deterioration in a mouse model of Alzheimer's disease. *J Neurosci*. 2008;28:6388-6392.
9. Liao F, Hori Y, Hudry E, et al. Anti-ApoE antibody given after plaque onset decreases Aβ accumulation and improves brain function in a mouse model of Aβ amyloidosis. *J Neurosci*. 2014;34:7281-7292.
10. Sevigny J, Chiao P, Bussière T, et al. The antibody aducanumab reduces Aβ plaques in Alzheimer's disease. *Nature*. 2016;537:50-56.
11. Swanson CJ, Zhang Y, Dhadda S, et al. DT-01-07: treatment of early ad subjects with BAN2401, an anti-Aβ protofibril monoclonal antibody, significantly clears amyloid plaque and reduces clinical decline. *Alzheimers Dement*. 2018;14:P1668-P1668.
12. Ni J, Taniguchi A, Ozawa S, et al. Near-infrared photoactivatable oxygenation catalysts of amyloid peptide. *Chem*. 2018;4:807-820.
13. Suzuki T, Hori Y, Sawazaki T, et al. Photo-oxygenation inhibits tau amyloid formation. *Chem Commun*. 2019;55:6165-6168.
14. Taniguchi A, Shimizu Y, Oisaki K, Sohma Y, Kanai M. Switchable photooxygenation catalysts that sense higher-order amyloid structures. *Nature Chem*. 2016;8:974-982.
15. Hori Y, Hashimoto T, Nomoto H, Hyman BT, Iwatsubo T. Role of apolipoprotein E in β-amyloidogenesis: isoform-specific effects on protofibril to fibril conversion of Aβ in vitro and brain Aβ deposition in vivo. *J Biol Chem*. 2015;290:15163-15174.
16. Saito T, Matsuba Y, Mihira N, et al. Single App knock-in mouse models of Alzheimer's disease. *Nat Neurosci*. 2014;17:661-663.
17. Jankowsky JL, Fadale DJ, Anderson J, et al. Mutant presenilins specifically elevate the levels of the 42 residue β-amyloid peptide in vivo: evidence for augmentation of a 42-specific γ secretase. *Hum Mol Genet*. 2004;13:159-170.
18. Arnold SE, Lee EB, Moberg PJ, et al. Olfactory epithelium amyloid-β and paired helical filament-tau pathology in Alzheimer disease. *Ann Neurol*. 2010;67:462-469.
19. Elmore MRP, Najafi AR, Koike MA, et al. Colony-stimulating factor 1 receptor signaling is necessary for microglia viability, unmasking a microglia progenitor cell in the adult brain. *Neuron*. 2014;82:380-397.
20. Tap WD, Wainberg ZA, Anthony SP, et al. Structure-guided blockade of CSF1R kinase in tenosynovial giant-cell tumor. *N Engl J Med*. 2015;373:428-437.
21. Nakamichi K, Saiki M, Kitani H, et al. Suppressive effect of simvastatin on interferon-β-induced expression of CC chemokine ligand 5 in microglia. *Neurosci Lett*. 2006;407:205-210.
22. Takenouchi T, Ogihara K, Sato M, Kitani H. Inhibitory effects of U73122 and U73343 on Ca2+ influx and pore formation induced by the activation of P2X7 nucleotide receptors in mouse microglial cell line. *Biochim Biophys Acta*. 2005;1726:177-186.
23. Tomita T, Maruyama K, Saido TCTC, et al. The presenilin 2 mutation (N141I) linked to familial Alzheimer disease (Volga German families) increases the secretion of amyloid β protein ending at the 42nd (or 43rd) residue. *Proc Natl Acad Sci U S A*. 1997;94:2025-2030.

24. Chiu YW, Hori Y, Ebinuma I, et al. Identification of calcium and integrin-binding protein 1 as a novel regulator of production of amyloid β peptide using CRISPR/Cas9-based screening system. *FASEB J*. 2020;34:7661-7674.
25. Ono M, Watanabe H, Kimura H, Saji H. BODIPY-based molecular probe for imaging of cerebral β-amyloid plaques. *ACS Chem Neurosci*. 2012;3:319-324.
26. Atwood CS, Perry G, Zeng H, et al. Copper mediates dityrosine cross-linking of Alzheimer's amyloid-β copper mediates dityrosine cross-linking of Alzheimer's. *Amyloid*. 2004;43:560-568.
27. Bondia P, Torra J, Tone CM, et al. Nanoscale view of amyloid photodynamic damage. *J Am Chem Soc*. 2020;142:922-930.
28. Frautschy SA, Cole GM, Baird A. Phagocytosis and deposition of vascular β-amyloid in rat brains injected with Alzheimer β-amyloid. *Am J Pathol*. 1992;140:1389-1399.
29. Majumdar A, Cruz D, Asamoah N, et al. Activation of microglia acidifies lysosomes and leads to degradation of Alzheimer amyloid fibrils. *Mol Biol Cell*. 2007;18:1490-1496.
30. Rogers J, Strohmeyer R, Kovelowski CJ, Li R. Microglia and inflammatory mechanisms in the clearance of amyloid β peptide. *Glia*. 2002;40:260-269.
31. Chu T, Tran T, Yang F, Beech W, Cole GM, Frautschy SA. Effect of chloroquine and leupeptin on intracellular accumulation of amyloid-beta (Aβ) 1-42 peptide in a murine N9 microglial cell line. *FEBS Lett*. 1998;436:439-444.
32. Gracanin M, Hawkins CL, Pattison DI, Davies MJ. Singlet-oxygen-mediated amino acid and protein oxidation: formation of tryptophan peroxides and decomposition products. *Free Radic Biol Med*. 2009;47:92-102.
33. Tomita M, Irie M, Ukita T. Sensitized photooxidation of histidine and its derivatives. Products and mechanism of the reaction. *Biochemistry*. 1969;8:5149-5160.
34. Uchida K, Kawakishi S. 2-Oxo-histidine as a novel biological marker for oxidatively modified proteins. *FEBS Lett*. 1993;332:208-210.
35. Wang C, Sun B, Zhou Y, Grubb A, Gan L. Cathepsin B Degrades Amyloid-β in Mice Expressing Wild-type Human Amyloid Precursor Protein. *Journal of Biological Chemistry* 2012; 287:39834-41.
36. Solé-Domènech S, Rojas A V, Maisuradze G G, Scheraga H A, Lobel P, Maxfield F R. Lysosomal enzyme tripeptidyl peptidase 1 destabilizes fibrillar Aβ by multiple endoproteolytic cleavages within the β-sheet domain. *Proc Natl Acad Sci USA* 2018; 115:1493-8.
37. Roher AE, Kokjohn TA, Clarke SG, et al. APP/Aβ structural diversity and Alzheimer's disease pathogenesis. *Neurochem Int*. 2017;110:1-13.
38. Deane R, Bell R, Sagare A, Zlokovic B. Clearance of Amyloid-beta peptide across the blood-brain barrier: implication for therapies in Alzheimers disease. *CNS Neurol Disord Drug Targets*. 2009;8:16-30.
39. Tarasoff-Conway JM, Carare RO, Osorio RS, et al. Clearance systems in the brain - implications for Alzheimer disease. *Nat Rev Neurol*. 2015;11:457-470.
40. Kikuchi K, Kidana K, Tatebe T, Tomita T. Dysregulated metabolism of the amyloid-β protein and therapeutic approaches in Alzheimer disease. *J Cell Biochem*. 2017;118:4183-4190.
41. Saido T, Leissring MA. Proteolytic degradation of amyloid β-protein. *Cold Spring Harb Perspect Med*. 2012;2:a006379.
42. Ihara H, Kakihana Y, Yamakage A, et al. 2-Oxo-histidine-containing dipeptides are functional oxidation products. *J Biol Chem*. 2019;294:1279-1289.
43. Traoré DAK, El Ghazouani A, Jacquamet L, et al. Structural and functional characterization of 2-oxo-histidine in oxidized PerR protein. *Nat Chem Biol*. 2009;5:53-59.
44. Nagashima N, Ozawa S, Furuta M, et al. Catalytic photooxygenation degrades brain Aβ in vivo. Sci Adv. 2021;7:eabc9750.
45. Busche MA, Wegmann S, Dujardin S, et al. Tau impairs neural circuits, dominating amyloid-β effects, in Alzheimer models in vivo. *Nat Neurosci*. 2019;22:57-64.